Indian Journal of Pure & Applied Physics
Vol. 60, March 2022, pp. 218-226

Influence of Thermal Annealing to Material Properties of TiO_2, ZnO, and TiO_2/ZnO Bilayer Films by Sol-Gel Method

Paulus Lobo Gareso[a*], Eko Juarlin[a], Heryanto Heryanto[a], Paulina Taba[b] & Didik Aryanto[c]

[a]Department of Physics, Hasanuddin University, Sulawesi Selatan 90245, Indonesia

[b]Department of Chemistry, Hasanuddin University, Sulawesi Selatan 90245, Indonesia

[c] Research Center of Physics, Indonesian Institute of Sciences (LIPI), Tengerang-Banten, Indonesia

Received 31 August 2021; accepted 24 February 2022

This study reported on the material properties of TiO_2, ZnO, and TiO_2/ZnO bilayer thin films fabricated by sol-gel spin coating technique after annealing. ZnO thin films were prepared by dissolving zinc acetate dehydrated into a solvent of ethanol and diethanolamine (DEA) was later added. Meanwhile, for TiO_2 films, titanium tetraisopropoxide (TTIP) was dissolved into ethanol and an acetate acid was added. Afterwards all film samples were annealed at different temperatures in the range of 400 – 600 ^oC for 60 minutes. For TiO_2/ZnO bilayer thin films, the structural properties showed that after annealing at 600 ^oC, the X-RD peak intensity was more pronounced compared to at 400 and 500 ^oC. This indicated that the amorphous phase of the films decreased after annealing at 600 ^oC. Furthermore, the crystallite sizes of the films increase as the annealing temperature increased to 600 ^oC, while the strain reduces at this temperature. In the case of (UV-Vis) spectroscopy, it was seen that after annealing the transmittance value of the TiO_2/ZnO bilayer increase. The band gap energy of the films consists of low and high energy. The low energy which is around 3.30 eV refers to the transitions of valence-conduction band in ZnO films and high energy was around 3.60 eV corresponding to the impurity transitions. In addition, the refractive index (n), the extinction coefficient (k), and the real and imaginary part of dielectric constant were determined from the transmittance and absorbance spectra results. Based on the SEM results indicate that there was no cluster in the surface of TiO_2/ZnO bilayer thin films.

Keywords: Sol-gel method, Thermal annealing, TiO_2/ZnO bilayer thin films

1 Introduction

The Combination of two semiconductor hetero-structures can increase the optical properties and the device performance of the semiconductors rather than a single semiconductor. In this study, ZnO and TiO_2 are the two metal-oxide semiconductors combined. ZnO is one of the II-VI compound semiconductors that have been received much attention due its outstanding optical and electrical properties. ZnO has a band gap energy of 3.3 eV[1,2] and a large exicton binding energy of 60 meV[3,4] which is widely used in thin film sensors[5], light emitting diodes (LED)[6] and photovoltaic devices[7]. In addition, it is a good candidate for photoanode in dye sensitized solar cells (DSSCs) application due to its low cost and non-toxicity. However, it has low energy conversion efficiency in photovoltaic performance. Therefore, to increase its device performance as the photoanode in DSSC application, TiO_2 and ZnO were combined, forming the ZnO/TiO_2 bilayer films which produce better photoanode properties.

On the other hand, TiO_2 material has wide band gap energy of 3.2 eV,[8] which is widely used in photo catalysts[9], applied as gas sensing in materials[10] and anti-reflection coatings[11]. It was also developed as a photoanode material because of its high performance in energy conversion efficiency. Therefore, it was used to improve the properties of ZnO and increase the performance of photoanode in DSSCs application. TiO_2 is classified into three phases of crystalline: anatase, rutile, and brookite[12,13]. The Rutile phase is the most stable phase and is usually obtained after annealing at temperature above 500 ^oC[12]. The optical band gap of TiO_2 is 3.0 and 3.2 eV for rutile and anatase crystalline phase respectively[13]. Mixed metal oxide TiO_2-ZnO nanostructures have been widely used as sensing gas materials[14] and the solar blind photoconductor[15].

There are many techniques that have been used to grow ZnO and TiO_2 thin film; radio frequency (RF) magnetron sputtering[16,17], molecular beam epitaxy (MBE)[18], spray pyrolysis[19,20] and sol gel spin coating method[21-23]. Among other methods, the sol-gel spin

*Corresponding author: (E-mail: pgareso@gmail.com)

coating method is one of the most attractive techniques used to fabricate the thin films due to its simplicity, inexpensive cost to characterize the structural and optical properties and the easy control of chemical compound.

In the present study, the structural and optical properties of TiO_2, ZnO, and TiO_2/ZnO bilayer thin film after annealing at different temperature are investigated. To achieve this, we first grow ZnO films on the glass substrates followed by TiO_2 on the top of ZnO thin film using sol-gel spin coating. The crystallite size and the strain of the films were estimated based on the X–ray diffraction results. Furthermore, the UV-Vis spectrophotometer was carried out to estimate the band gap energy of the films. The refractive index (*n*), the extinction coefficient, and the real and imaginary part of dielectric constant were also characterized based on the transmittance and absorbance results. The surface morphology of the films was observed using the scanning electron microscopy (SEM), and from the SEM results we estimate the thickness of the films.

2 Experimental detail

2.1 Synthesis of ZnO, TiO_2, and TiO_2/ZnO bilayer films

ZnO thin film was prepared using zinc acetate dehydrate ($Zn(CH_3COO)_2.2H2O$) as a starting material. First, zinc acetate dehydrate was dissolved into 1.5M of ethanol and diethanolamine (DEA) as a solvent and stabilizer, respectively. The solvent was stirred on the magnetic hotplate for 30 minutes and the sol-gel was growth on glass substrate with the speed rate of 3000 rpm for 30 seconds. Next, the films were heated on the hot plate for 30 minutes to evaporate the mixture and unwanted organic residuals. After fabricating the ZnO films as a first layer, the TiO_2 films were fabricated subsequent on the top of ZnO films. 1.5 ml titanium tetraisopropoxide (TTIP) was dissolved into 10 ml ethanol and 0.1 ml acetate acid was added. These solvent were stirred on the magnetic hotplate at 80 ^oC for 5 hours. Afterwards, the sol-gel was coated on a glass substrate by spin coating with a speed rate of 3000 rpm for 30 seconds and was heated on the hotplate for 30 minutes to remove the undesireable mixture from the surface.

Prior to the fabrication of ZnO/TiO_2 bilayer thin films on the glass substrate, it was cleaned with HCL to remove the unwanted particles from its surface. The ZnO solution was first deposited on the glass substrate to form the ZnO film. Afterwards, it was heated on the hotplate at 300 ^oC to evaporate the solvent from the surface. Furthermore, the second layer of TiO_2 was deposited on the ZnO films to form the ZnO/TiO_2 bilayer thin films. These layers were heated on the hotplate to evaporate the remaining residual in the films. The ZnO/TiO_2 bilayer films were finally inserted into the furnace to anneal the samples at different temperatures from 400 to 600 ^oC for 60 minutes.

2.2. Materials characterization

X-ray diffraction (X-RD) measurement was recorded to study the crystallite size and the strain of ZnO, TiO_2 and TiO_2/ZnO using Cu Kα radiation. The recorded of diffraction angle was varied from 20^o to 70^o. The voltage and the current of X-RD were kept a constant at 40 kV and 30 mA, respectively with the speed rate of X-RD was 2^o/min. The crystallite size and the strain of the films were estimated based on the X-RD results using Debye-Scherrer equation and William-Hall methods. We used SEM to evaluate the surface morphology of the thin films. Furthermore, the UV-Vis optical transmittance spectroscopy was carried out to estimate the band gap energy of single layer ZnO, TiO_2 and TiO_2/ZnO bilayer thin films using a single beam UV-Vis spectroscopy with a wavelength range of 300 – 800 nm. Further investigation of optical properties such as the refractive index (n), the extinction coefficient (k) and the dielectric were determined using the UV-Vis results.

3 Results and Discussion

3.1 Structural characterization

Figure 1 (a,b) depict the recorded X-RD spectra of a single layer TiO_2 and ZnO film after annealing at different temperatures from 300 to 600 ^oC for 60 minutes. For TiO_2 thin films, The X-ray diffraction patterns were clearly seen after annealing the films at 300 ^oC. The diffraction angle of 2θ at the X-RD spectra of TiO_2 films were observed at 25.41, 37.97 and 48.31^o that corresponded to the reflection of (101), (004) and (200), respectively. After annealing the films at 600 ^oC, the 2θ was shifted to the right at 25.61, 38.08 and 48.51^o, respectively. The strong peak was located at 2θ=25.41^o showing an anatase phase with preferential orientation of (101) plane (JCPDS card no 21-1272). Furthermore, previous studies on TiO_2 films showed that the preferential growth of

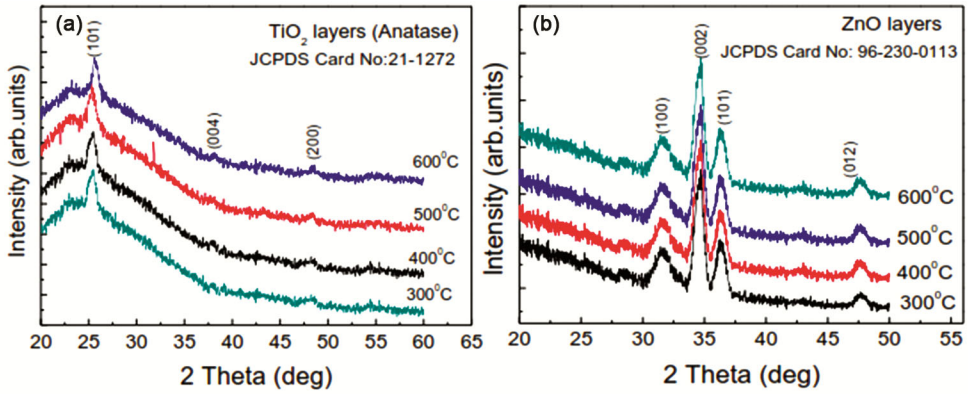

Fig. 1 — (a) X-RD patterns of TiO_2 thin films after annealing with different temperatures from 300 °C to 600 °C for 60 minutes and (b) shows the X-RD patterns of ZnO thin films after annealing with different temperatures from 300 to 600 °C for 60 minutes.

TiO_2 was in (101) plane direction and was categorized as anatase crystalline phase which was confirmed in the results obtained[24,25]. Conversely, the recorded X-RD spectra of ZnO films Fig 1(b) annealing at various temperatures revealed four well defined X-RD maxima at diffraction angle of 31.62, 34.72, 36.27 and 47.57° (JCPDS card No: 96-230-0113) that were attributed to reflections plane of (100), (002), (101) and (012), respectively. These crystal planes corresponded to the hexagonal wurtzite phase. In addition, the preferential growth of ZnO films were in (002) direction since its intensity was higher than that of other plane. This result was in agreement with the previous studies where the preferential growth of ZnO films was in (002) direction[5,26].

Figure 2 shows the X-RD curves of TiO_2/ZnO bilayer thin films after annealing at different temperatures from 400 to 600 °C. As shown in this figure, after annealing at 400 °C, the intensity of recorded X-RD peak is very weak. However, after annealing at 600 °C the X-RD peak of TiO_2/ZnO bilayer thin film was clearly observed with higher intensity than that 400 and 500 °C, more pronounced X-RD peaks appeared at this annealing temperature. Furthermore, the diffraction angle 2θ of 26.61°, 48.18° assigned to (101) and (200) plane belonged to the TiO_2 anatase phase. Meanwhile, ZnO X-RD peaks were observed at 2θ=32.51°, 37.09°, 56.84°, 63.15° and 68.38° assigned to the planes of (100), (002), (101), (110), (103), and (201), respectively. A very strong X-RD peak in ZnO film was observed at the diffraction angle of 35.13° represented by (002) plane. In addition, it was discovered that the diffraction angle of 56.84, 63.15 and 68.38° were also represented by the TiO_2 rutile phase of (220), (130) and (112) planes (JCPDS card no 21-1272). It is

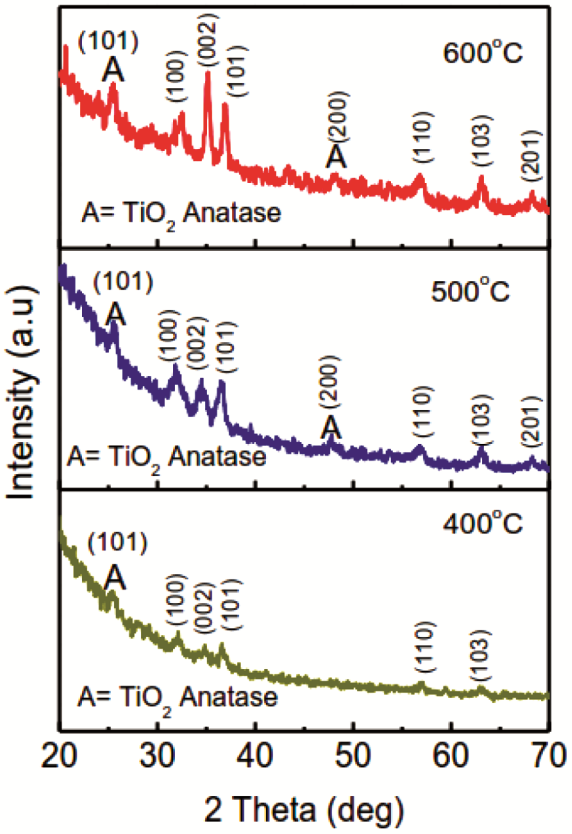

Fig. 2 — X-RD spectra of TiO_2/ZnO bilayer thin films after annealing at different temperatures from 400°C to 600°C for 60 minutes. *Note*. A symbol refers to TiO_2 anatase phase.

interesting to note that the X-RD peak related to (004) plane of TiO_2 anatase phase which appeared in the single layer of TiO_2 were not detected in bilayer TiO_2/ZnO bilayer thin films indicating the reduction of TiO_2 phase fraction in this layer. Similar results have also been reported in the previous study by Kheiri *et al.*[27] and Choi *et al.*[28]. They showed that

there was a significant reduction in the TiO_2 fraction when the layers of ZnO were deposited on TiO_2 as a result of the instability in the growth of the TiO_2 layer on ZnO. It was observed that there was an improvement in the crystalline bilayer TiO_2/ZnO bilayer thin films after annealing at 600 °C which was indicated by an increase in the X-RD intensity. The results confirmed in the previous studies in which the intensity of TiO_2/ZnO bilayer thin films after annealing at high temperature was inversely proportional to the amorphous phase[29,30].

The crystallite size of the bilayer TiO_2/ZnO bilayer thin films can be estimated using the Debye-Scherrer equation as follows[31],

$$D = \frac{0.9\lambda}{\beta_{hkl} cos\theta} \quad \ldots (1)$$

Where λ is the X-ray wavelength (λ = 1.5406 Å), β_{hkl} is the full width at half-maximum (FWHM) and θ is the Bragg angle, respectively. In addition, William-Hall method (Uniform Deformation Method=UDM) was used to calculate the crystallite size and the strain of TiO_2/ZnO bilayer thin films in the following equation[32,33].

$$\beta_{hkl} cos\theta = \frac{k\alpha}{D} + (4\varepsilon\, sin\theta) \quad \ldots (2)$$

It is assumed in the equation (2), that the strain is uniform. The fitted line of $\beta_{hkl}\ cos\theta$ to $4sin\theta$ give results the slope and *y*-intercept that represents to the strain and the crystalline size of the samples. The crystallite size and the strain that were calculated from equation (1) and (2) are tabulated in Table 1. Both the Debye-Scherrer and William-Hall method (UDM) showed that the crystallite size of TiO_2/ZnO bilayer thin film increased after annealing at high temperature indicating it's improvement as a result of the increasing X-RD intensity. Meanwhile, the reduction of the strain took place after annealing at 600 °C. Similar results have been published by Khan *et al*.[30] and Kheiri *et al*.[27]. They showed that the crystallite size and X-RD intensity were directly proportional to the number of ZnO/TiO_2 layer. Therefore, increasing the intensity as a result of the improvement of the crystalline size would reduce stress on the films.

3.2. Surface morphology

The surface morphology of TiO_2/ZnO bilayer thin films was presented by scanning electron microscopy (SEM) image as shown in Fig. 3. The films exhibiting a smooth surface with some small dots which were not well distributed on the surface were observed. Meanwhile, some cracks on the surface of the films were also observed. Furthermore, through SEM, the thickness of TiO_2/ZnO bilayer thin films films that were used to obtain the optical band gap energy was determined. Based on SEM results, the total thickness of the films was 0.98 μm.

3.3 Optical characterization

3.3.1 Transmittance and absorbance

UV-Vis spectroscopy was used to characterize the optical properties of deposited TiO_2, ZnO, and

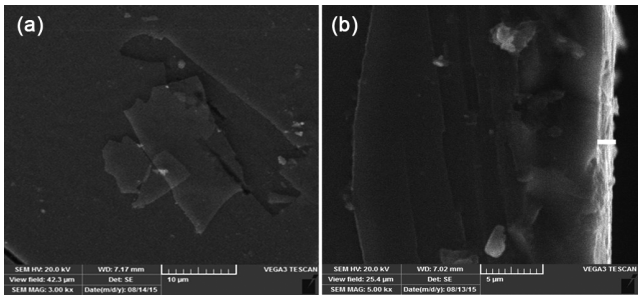

Fig. 3 — (a) SEM image of TiO_2/ZnO bilayer thin films after annealing at 600 °C, (b) cross section of TiO_2/ZnO bilayer thin films.

Table 1 — The structural parameters of bilayer thin films after annealing at various temperatures. *Note*. Asterisk (*) symbol refers to TiO_2 anatase phase

Annealed samples (TiO_2/ZnO)	2θ (deg)	FWHM (deg)	(hkl)	Scherer Method [31]		William Hall Method [32,33] Uniform Deformation Method	
				Size (nm)	Strain ($x10^{-3}$)	Size (nm)	Strain ($x10^{-3}$)
500 °C	25.41	0.51	(101)*	11.63	10.9	6.58	6.4
	31.86	1.08	(100)				
	34.49	0.92	(002)				
	36.44	0.68	(101)				
	48.33	0.56	(200)*				
600 °C	26.61	0.61	(101)*	14.36	7.9	19.30	2.1
	32.51	0.58	(100)				
	35.13	0.62	(002)				
	37.09	0.58	(101)				
	48.18	0.68	(200)*				

TiO_2/ZnO bilayer thin films. Fig. 4 depicts the transmittance and absorbance spectra of ZnO and TiO_2 films after annealing at 400 °C and 500 °C, respectively. The transmittance value of TiO_2 film after annealing at 400 °C was around 55 % which was lower compared to the transmittance value after annealing at 500 °C. The transmittance value of TiO_2 after annealing 500 °C was around 85 % in visible regions. Meanwhile, for ZnO film, the transmittance value after annealing 400 °C was around 45 % which increased to 75 % after annealing at 500 °C.

Figure 5 shows the transmittance and absorbance spectra of TiO_2/ZnO bilayer films. The transmittance value of the films was around 75 % - 85 % after annealing at 400 °C. This value decreased to about 60 – 65 % when the film was annealed at 500 °C and increased to 70-75 % after annealing at 600 °C. Furthermore, the absorbance spectra may be divided into three regimes. Firstly, the strong absorbance at $\lambda = 305$ nm, absorbance shoulder region near the band edge for $345 \leq \lambda \leq 370$ nm and the weak absorbance for $\lambda \geq 400$ nm. The transmittance and absorbance spectra of TiO_2/ZnO bilayer films also presented some exciton absorption features depending on the annealing temperatures which can be seen in Fig. 5. After annealing at 400, 500 and 600 °C, the exciton absorption showed at 362 nm, 367 nm and 369 nm, respectively, indicating an increase at 600 °C. These values were in close range with the exciton absorption of bulk ZnO which was located at 373 nm[34]. Ivanova *et al*. have reported the existing of the exciton absorption in the ZnO/TiO_2 deposited film used sol-gel method. The exciton absorption peak was assigned at the wavelength of 362 and 363 nm after annealing at 400 and 500 °C. These numbers were very close to results obtained from this study. The band gap energy of the films was estimated by extrapolation of the linier relationship between $(\alpha h\upsilon)^2$ and $h\upsilon$ according to the equation[35].

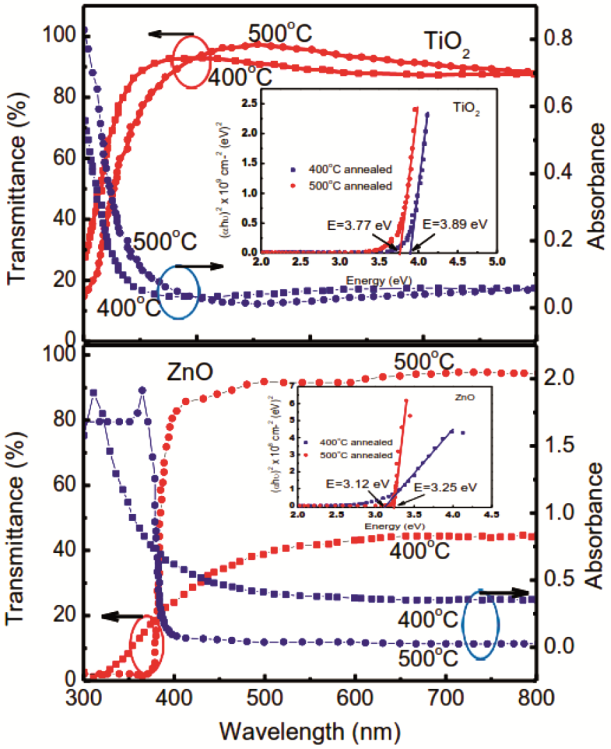

Fig. 4 — The transmittance and absorbance spectra of ZnO and TiO_2 thin films after annealing at 400 °C and 500 °C. The band gap energy of ZnO and TiO_2 thin films are also depicted (inset figure).

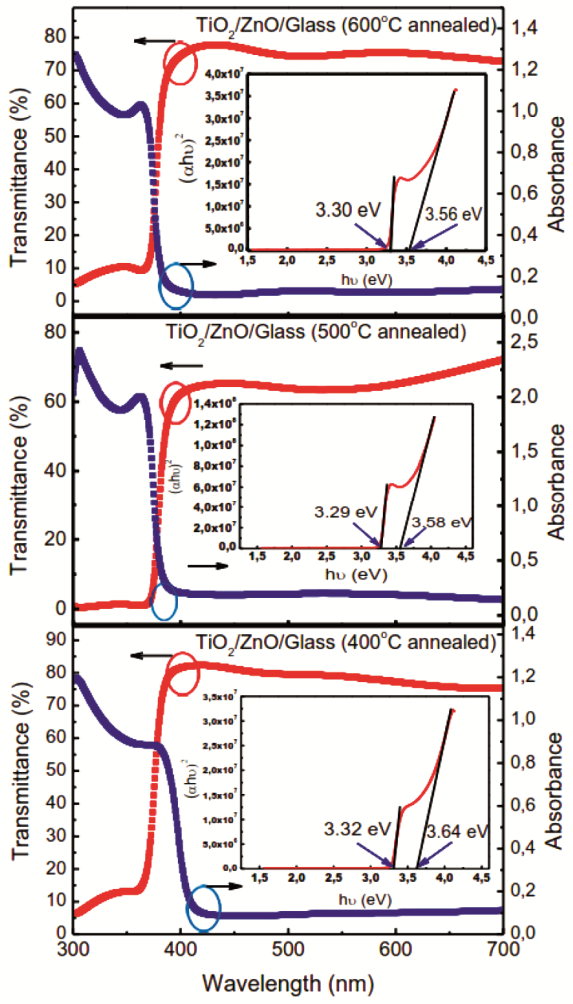

Fig. 5 — The transmittance and absorbance spectra of TiO_2/ZnO bilayer thin films after annealing at various temperatures from 400 °C to 600 °C for 60 minutes. The inset figure shows the band gap energy of TiO_2/ZnO bilayer thin films before and after annealing with different temperatures from 400 to 600 °C.

$$(\alpha h\upsilon)^2 = A\left(h\upsilon - E_g\right) \quad \ldots (3)$$

$$\alpha = 2.303\ x\ \left(\frac{Abs}{d}\right) \quad \ldots (4)$$

Where α is the absorption coefficient, *Abs* is the optical absorbance, *d* is the thickness of the film, *hυ* is the energy and E_g is the band gap energy and *A* is a constant.

Furthermore, the inset Fig. 4, 5 shows the plot of $(\alpha h\upsilon)^2$ to photo energy (*hυ*) for TiO_2, ZnO and TiO_2/ZnO bilayer films after annealing at different temperatures from 400 °C to 600 °C for 60 minutes. The band gap energy of the films was obtained by extrapolating the linier part of $(\alpha h\upsilon)^2$ against energy (*hυ*). For TiO_2 films, as shown in inset Fig. 4, the band gap energy of TiO_2 films were estimated around 3.89 eV that annealed at 400 °C, which reduced to about 3.77 eV (500 °C annealed). These values were higher than the E_g bulk TiO_2. The large difference between TiO_2 film and TiO_2 bulk was probably due to the grain size and the crystalline structure of thin film and bulk[36,37]. In addition, The E_g values were slightly larger compared with studies reported by Kheirei *et al*.[27], and Ivanova *et al*.[29]. According to Kheiri *et al*. the estimated value of the optical band gap energy of TiO_2 films were 3.756 eV and 3.677 eV after annealing at 400 °C and 600 °C, respectively. Similar behaviour was reported by Ivanova *et al*, the E_g value had 3.74 eV (400 °C) and 3.73 eV (500 °C). However, the results obtained from this study are in agreement with the previous study reported by Quinones *et al*[38]. Meanwhile, in the case of ZnO film, the inset Fig. 4 displayed the optical band gap energy of ZnO after annealing at 400 °C and 500 °C. The estimated E_g value for ZnO films were 3.12 eV (400 °C) and 3.25 eV (500 °C). These value were relatively lower than that of previous results[1,2].

The band gap energy of TiO_2/ZnO bilayer thin film in inset Fig. 5 has two energy values which are the low and the high energy band gap. These results were quite different when compared with the previous studies that have been carried out in estimating the effective bandgap energy based on derivation from the Touc Plot where only one effective band gap energy was observed in their studies[27,29]. The first energy (E_1) refers to band to band transition in ZnO films also known as the forbidden gap energy having a value range of 3.29 – 3.32 eV after annealing at 400 °C to 600 °C (Table 2). This energy value referred to the bulk ZnO that have been published in previous studies[1,2]. In addition, this effective band gap energy was almost similar to the TiO_2 anatase phase of 3.2 eV which was confirmed in the previous studies[8]. The second energy E_2 had a value ranging from 3.56 – 3.64 eV after annealing at 400, 500 and 600 °C, respectively. The E_g value in the combination of TiO_2 and ZnO was lower than the single layer TiO_2 film. The reduction of E_g value in TiO_2/ZnO bilayer thin films was probably due to the penetration of Ti^{+4} into ZnO layer that resulted in the reduction in the phase fraction of TiO_2 after it was deposited on top of the ZnO. This created a new binding energy having lower optical band gap energy in comparison to TiO_2 single layer. This explanation was confirmed from the X-RD results where there was a reduction in both X-RD intensity and the plane corresponded to the TiO_2 single layer as a result of the reduction in the phase fraction of TiO_2 layer. Furthermore, similar behaviour was also observed by Kheire *et al*. where they discovered that reducing the TiO_2 phase fraction increased the density of impurity. In addition, the value of energy E_2 was higher than previous result that has been published by Kheiri *et al*.[27]. They reported that the effective band gap energy was in the range of 3.22 – 3.26 eV after annealing at various temperatures from 400 °C to 600 °C which was very close to the pure ZnO. In Kheiri *et al,* ZnO was the top layer of ZnO/TiO_2/glass. However, the results of effective band gap energy obtained in this study were lower than that reported by Ivanova *et al*.[29]. They had estimated that the effective band gap energy was in the range of 3.88 – 3.91eV with various annealing temperatures from 400 – 600 °C. Previous study by Hernandes *et al*. reported that the effective band gap energy of Zn_2TiO_2 was 3.7 eV[39]. The effective band gap energy (E_2) observed in this study was almost similar to that reported by Hernandes.

Table 2 — The band gap energy and refractive index (*n*) of TiO_2, ZnO, TiO_2/ZnO bilayer thin films derived from UV-Vis spectroscopy.

Material	Annealing temperature	*Eg* (eV)	Refractive index (*n*)
TiO_2	400 °C	3.89	1.73
	500 °C	3.77	1.72
ZnO	400 °C	3.12	1.26
	500 °C	3.25	2.19
	400 °C	E_1= 3.32	2.21
		E_2= 3.64	2.63
TiO_2/ZnO	500 °C	E_1= 3.29	2.36
		E_2= 3.58	2.94
	600 °C	E_1= 3.30	2.16
		E_2= 3.56	2.68

3.3.2. Refractive index, extinction coefficient and dielectric constant

The other important optical parameter was the refractive index (n) and the extinction coefficient (k) of the film. The refractive index (n) corresponded to the polarizability of ion and local field inside the film. The refractive index (n) and extinction coefficient (k) were estimated using equation[40].

$$n = \frac{(1+R)+2\sqrt{R}}{(1-R)} \quad \ldots (5)$$

$$R = 1 - (Te^{A})^2 \quad \ldots (6)$$

$$k = \frac{\alpha\lambda}{4\pi} \quad \ldots (7)$$

Where R is the reflectance of the film that is calculated from the transmittance (T), A is the absorbance, α is the absorption coefficient and λ is the wavelength. The refractive index (n) and the extinction coefficient (k) as a function of wavelength for single layer TiO_2, ZnO and TiO_2/ZnO bilayer thin films were displayed in Fig. 6, 7. In Fig. 6, the refractive index (n) of TiO_2 annealed at 400 °C was higher than that annealed at 500 °C. In addition, the refractive index (n) reduced significantly from 2.6 (λ=300 nm) to 1.1 (λ=412 nm) after annealed at 500 °C and became constant at λ>425 nm. For ZnO films, similar behaviour in TiO_2 was observed in ZnO film where the refractive index (n) tended to be constant at λ>450 nm. Meanwhile, for the extinction coefficient (k), both in TiO_2 and ZnO were lower than that of the refractive index (n). For TiO_2/ZnO bilayer thin films (see Fig. 7), the refractive index (n) was in the range of 2.6 – 3.0 at a wavelength of less than 360 nm. Subsequently, it reduced quite significantly to 1.36, 1.56 and 1.27 at wavelength of 394 nm (3.15 eV) after annealing at 400 °C, 500 °C and 600 °C, respectively. The effective band gap energy at 3.30 eV and 3.56 eV were assigned to the refractive index (n) of 2.16 and 2.68 (See Table 2). In comparison with the previous studies[41], the refractive index (n) of polycrstalline ZnO film and TiO_2 were assigned 2.22 and 2.32, respectively. Ivanova et al. showed that the refractive index (n) of ZnO/TiO_2 was 2.19 which was lower than results obtained from this study. Meanwhile, the extinction coefficient (k) was lower than that of the refractive indices for all films after annealing at 400 °C, 500 °C and 600 °C, respectively.

Furthermore, the fundamental excitation spectrum of the films was described by means of a frequency dependent on the complex electronic dielectric constant which was defined as $\varepsilon = \varepsilon_r + i\varepsilon_i$, where ε_r and ε_i are the real and imaginary part of dielectric constant, respectively that corresponded to the refractive index n and the extinction coefficient k according to equation[42].

$$\varepsilon_r = n^2 - k^2 \quad \ldots (8)$$

$$\varepsilon_i = 2nk \quad \ldots (9)$$

Figure 8 shows the real ε_r and imaginary part ε_i of dielectric constant of bilayer TiO_2/ZnO bilayer thin films after annealing at 400 °C to 600 °C for 60

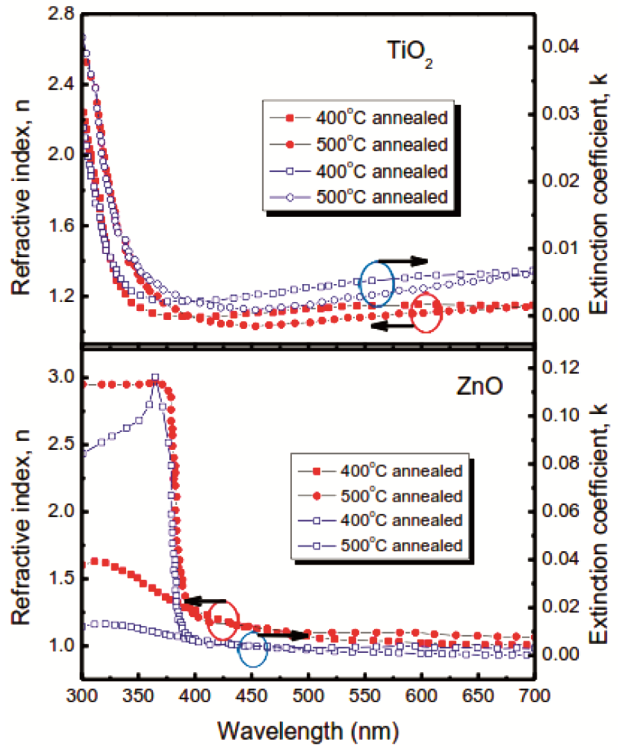

Fig. 6 — The refractive index (n) and the extinction coefficient (k) of TiO_2 and ZnO after annealing at 500 °C and 600 °C for 60 minutes.

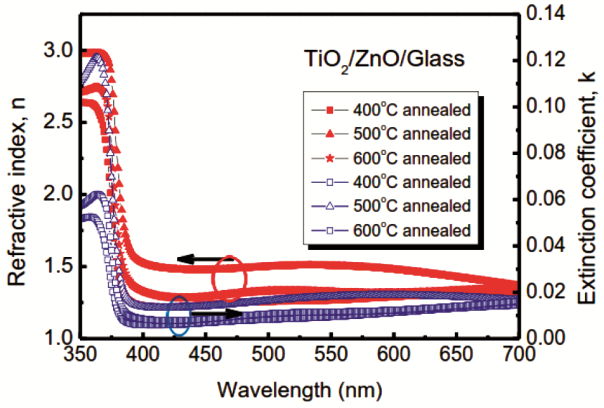

Fig. 7 — The refractive index (n) and the extinction coefficient (k) of TiO_2/ZnO after annealing at various temperatures from 400 °C to 600 °C for 60 minutes.

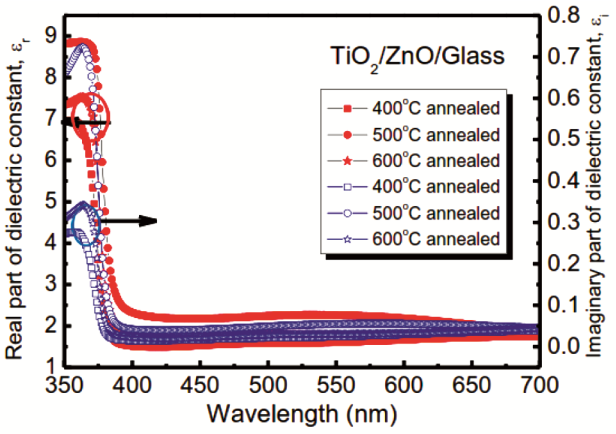

Fig. 8 — The real (ε_r) and imaginary (ε_i) part of dielectric constant of TiO_2/ZnO bilayer thin films after annealing at various temperatures from 400 °C to 600 °C for 60 minutes.

minutes. The variation of real and imaginary part of dielectric constant was inversely proportional to the wavelength, reaching a maximum at the wavelength of around 362 nm and vice versa. In addition, the imaginary part of dielectric constant was similar in behaviour to the real dielectric constant which shows that there was a maximum dielectric constant with a certain value of wavelength.

4 Conclusion

Thin films of metal oxide TiO_2, ZnO and bilayer TiO_2/ZnO bilayer thin films have been successfully synthesized and characterized using X-ray diffraction, SEM and UV-Vis spectroscopy measurements after annealing at different temperature in the range 400 °C – 600 °C. From X-RD results obtained, it was observed that the X-RD peak intensity in TiO_2/ZnO was more pronounced in the films after annealing at 600 °C compared to the films annealed at 400 and 500 °C, respectively. Furthermore, the optical properties of TiO_2/ZnO bilayer thin films showed a high value transmittance which was around 80% in the visible regions after annealing at 600 °C. The effective optical band gap energy of mixed TiO_2 and ZnO which was derived from Touch plot gave two regions at low and high energy. In addition, the optical band gap energy of the TiO_2 layer was higher than that of the mixed TiO_2 and ZnO layers. The refractive index (n), the extinction coefficient (k) and the dielectric constant showed similar behaviour in the single layer and mixed layer. Based on the optical characterization of TiO_2, ZnO and TiO_2/ZnO bilayer, these materials were suitable for application in optoelectronic devices.

Acknowledgement

P.L. Gareso expresses gratitude to the higher education of Indonesia (KEMENRISTEK-BRIN) and LP2M-UNHAS for the financial support in the Basic Research Scheme under contract number of 752/UN4.22/PT.01.03/2021.

References

1 Rai R C, Guminiak M, Wilser S, Cai B & Nakarmi M L *J, Appl Phys*, 111 (2012) 073511.
2 Kamaruddin S A, Chan K Y, Yow H K, Sahdan M Z, Saim H & Knipp D, *Appl Phys A*, 104 (2011) 263.
3 Inamdar S I, Ganbavle V V & Rajpure K Y, *Superlatt Microstruct*, 76 (2014) 253.
4 Aksoy S & Caglar Y, *Superlatt Microstruct*, 51 (2012) 613.
5 Patil N B, Nimbalkar A R & Patil M G, *Mater Sci Eng B*, 227 (2018) 53.
6 Choi Y S, Kang Y W, Hwang D K & Park S J, *IEEE Trans Electron Dev*, 57 (2010) 26.
7 Falcao V D, Miranda D O, Sabino M E L, Moura T D O, Diniz A S A C, Cruz L R & Branco J R T, *Prog Photovolt Res*, 19 (2011) 149.
8 Tian J, Chen L, Dai J, Wang X, Yin Y & Wu P, *Ceram Int J*, 35 (2009) 2261.
9 Zhang M, An T, Liu X, Hu X, Sheng G & Fu J, *Mater Lett*, 64 (2010) 1883.
10 Gui Y, Li Sh & Li Ch, *Microelectron J*, 39 (2008) 1120.
11 Vaezi M R, *Mater Process Technol*, 205 (2008) 332.
12 Abozovic N D, Mirenghi L, Jamkovic I A, Bibic N, Sojic D V, Abramovic B F & Cmor M L, *Nanoscale Res Lett*, 4 (2009) 518.
13 Paola A D, Bellardita M & Palmisano, *Catalysts*, 3 (2013) 36.
14 Lin Y, Wei J G C, Chii Y F, Ju W L, James W H, Tunney J & Ho K C, *Sens Actua B*, 157 (2011) 361.
15 Lakhotia G, Umarji G, Jagtap S, Rane S, Mulik U, Amalnerkar D & Gosavi S W, *Mater Sci Eng B*, 168 (2010) 66.
16 Jasmati A K & Bassam A, *Mater Res*, 21 (2018) 1.
17 Simionescu O C, Romanitan C, Tutunaru O, Ion V, Buiu O & Avram A, *Coating*, 9 (2019) 3.
18 Opel M, Geprags S, Althammer M, Brenninger T & Gross R, *J Phys D: Appl Phys*, 47 (2014) 034002.
19 Lehraki N, Aida M S, Abed S, Attaf N, Attaf A & Poulain M, *Curr Appl Phys*, 12 (2012) 1283.
20 Ennaoui A, Sankapal B R, Skryshelevsky V, Ch M & Lux-Steiner, *Sol Energy Mater Sol Cells*, 90 (2006) 1533.
21 Gareso P L, Musfitasari & Juarlin E, *J Phys Conf Ser*, 979 (2018) 012060.
22 Raoufi D & Raoufi T, *Appl Surf Sci*, 255 (2009) 5812.
23 Ghamsari M S & Bahramian A R, *Mater Lett*, 62 (2008) 361.
24 Kao M C, Chen H Z & Young S L, *Appl Phys A: Mater Sci Process*, 97 (2009) 469.
25 Dussan A, Bohórquez A & Quiroz H P, *Appl Surf Sci*, 424 (2017) 111.
26 Nimbalkar A R & Patil M G, *Physica B*, 527 (2017) 7.
27 Kheiri F, Soleimanian V, Ghasemi M & Mokhtari A, *Mater Sci Semicon Proc*, 121 (2021) 105462.
28 Choi W S, Kim E J, Seong S G, Kim Y S, Park C & Hahn S H, *Vacuum*, 83 (2009) 5.

29 Ivanova T, Harizanova A, Koutzarova T & Vertuyen B, *J Non-Cryst Solids*, 357 (2011) 2840.
30 Khan M I, Imran S, Saleem S M & Rehman S U, *Res Phys*, 8 (2018) 249.
31 Fallah H R, Ghasemi M, Hassanzadeh A & Steki H, *Physica B*, 373 (2006) 274.
32 Biju V, Sugathan N, Vrinda V & Salini S L, *J Mater Sci*, 43 (2008) 1175.
33 Pandiyarajan T & Karthikeyan B, *J Nano Res*, 14 (2012) 647.
34 Shinde R, Gujar T P & Lokhande C D, *Sol Energy Mater Sol Cells*, 91 (2007) 1055.
35 Tauc J, Grigorovichi R & Vancu A, *Phys Status Solidi B*, 15 (1996) 627.
36 Gonza'lez-Leal J M, Prieto-Alcon R, Angel J A & Marquez E, *J Non-Cryst Solids*, 315 (2003) 134.
37 Sheng Y, Liang L, Xu Y, Wu D & Sun Y, *Opt Mater*, 30 (2008) 1310.
38 Quiñonez C, Vallejo W & Gordillo G, *Appl Surf Sci*, 256 (2010) 4065.
39 Mayen-Hernandez S A, Torres-Delgado G, Castanedo-Perez R, Marquez Marin J, Gutierrez-Villarreal M & Zelaya-Angel O, *Sol Energy Mat Sol Cells*, 91 (2007) 1454.
40 Raj K R & Murogakoothan P, *Optic*, 123 (2012) 1082.
41 Yang C, Fan H, Xi Y, Chen J & Li Z, *Appl Surf Sci*, 254 (2008) 2685.
42 Jacob A A, Balalkrishnan L, Meher S R, Shambawi K & Alex Z C, *J Alloy Compd*, 695 (2017) 3753.